Meteorol. Atmos. Phys. 44, 29–41 (1990)

Meteorology and Atmospheric Physics

551.515.5:551.513

Institute of Geoscience, University of Tsukuba, Tsukuba, Japan

Impact of Indian Monsoon on the Coupled Atmosphere/Ocean System in the Tropical Pacific

T. Yasunari

With 9 Figures

Received May 19, 1989
Revised September 25, 1989

Summary

This study addresses the relationship between the Indian summer monsoon (ISM) and the coupled atmosphere/ocean system in the tropical Pacific on the interannual time scales. High positive correlations are found between ISM rainfall and both mixed layer sea water temperature (SWT) and sea surface temperature (SST) anomalies of the tropical western Pacific in the following winter. Negative correlations between ISM rainfall and SST in the central/eastern Pacific also appear to be most significant in the following winter. These parameters are correlated with each other mainly on a biennial time scale. Lag-correlations between the zonal wind and SST along the the equatorial Pacific show that the westerly (easterly) surface wind stress anomalies over the central/western Pacific are greatly responsible for the formation of negative (positive) SST/SWT anomalies in the western Pacific and positive (negative) SST/SWT anomalies in the central/eastern Pacific. Furthermore, it is evidenced that these lag-correlations are physically based on the anomalies in the large-scale convection over the Asian monsoon region and the associated east-west circulation over the tropical Pacific, which first appear during the Indian summer monsoon season and evolve during the following autumn and winter.

These results strongly suggest that the Asian summer monsoon may have an active, rather than a passive, role on the interannual variability, including the ENSO events, of the coupled atmosphere/ocean system over the tropical Pacific.

1. Introduction

Since the early part of this century (Walker and Bliss, 1932), many studies have been done on the relationship between the Indian summer monsoon (ISM) and the El Niño/Southern Oscillation (ENSO) phenomena. In recent years, ENSO has become a matter of great interest as an atmosphere/ocean interaction which affects the interannual variability of global climate. In particular, some works have stressed the role of ENSO in the interannual variability of the Indian monsoon. Nicholls (1984), for example, adopted SST anomalies in the Indonesian-north Australian area as a predictor of the Indian monsoon rainfall. Rasmusson and Carpenter (1983) suggested that SST anomalies in the eastern Pacific can be a potential predictor for the Indian monsoon rainfall. Angell (1981), on the other hand, noted that SST anomalies in the equatorial eastern Pacific during fall and winter are highly correlated with the preceding Indian monsoon rainfall. Shukla and Paolino (1983) also stressed the influence of the Indian monsoon on ENSO, pointing out that Indian monsoon rainfall anomalies are highly correlated with sea-level pressure anomalies at Darwin (as an index of the Southern Oscillation) in the following autumn and winter. Global analyses of sea level pressure (Barnett, 1985) and atmospheric circulation fields (Yasunari, 1987) also suggested the role of the Indian monsoon on the evolution of the ENSO cycle. These studies showed distinct signatures over the Indian Ocean and the Eurasian

continent which preceded the ENSO events in the equatorial eastern Pacific.

On the other hand, oceanographical evidence (Wyrtki, 1975, etc.) suggests the importance of the thick and warm oceanic mixed layer in the equatorial western Pacific as an origin of the El Niño events in the eastern Pacific. Recent oceanic model studies with observed wind forcing (White et al., 1987; Miyakoda et al., 1987) also showed that an anomalously high heat content in the surface layer of the western tropical Pacific is formed one year prior to a mature ENSO event by strong easterly wind stress over the tropical north Pacific. Very recently, Yamagata and Masumoto (1989) demonstrated, by use of a simple atmosphere/ocean coupled model, that an ENSO event evolves automatically on the condition that warm SST and positive anomaly of oceanic heat content (OHC) covers all the equatorial Pacific, as was pointed out by Zebiak and Cane (1987). They have also suggested, however, that this condition is prepared only when the atmospheric westerly bursts and positive OHC anomaly in the western Pacific are coupled. Pazan et al. (1986) noted the role of off-equatorial Rossby waves, which propagate westward from the central Pacific, on the anomalously high dynamic height in the western Pacific. In view of this, the important question may be what actually controls the heat content and dynamic height anomalies of the oceanic mixed layer in the tropical western Pacific, and how the Asian monsoon activity is related to these anomalies. This may give a clue as to what the mechanism of the ENSO cycle is.

The present paper attempts to solve these problems based on observational data. Some atmospheric and oceanic key parameters will be systematically examined by lag-correlation and composite techniques, particularly relevant to Indian monsoon activity. Some apparent evidences will be presented that the variability of the Indian summer monsoon and the associated convective activity over the Asian monsoon region play a crucial role in the ENSO cycle.

2. Data

Monthly, gridded 15 year (1970–1984) SST data compiled at NOAA are used in the present study. The 2° × 2° lat./lon. grid data for the Pacific basin were converted into areal mean data of 4° × 4° lat./lon. blocks. January and July SWT profile data along 137 °E for the 19 years (1967–1985), regularly observed by the research vessel Ryofu-Maru of the Japan Meteorological Agency (JMA), are also utilized. This data set is invaluable for examining the depth and temperature of the oceanic mixed layer in the tropical western Pacific. ISM rainfall (June to September) index (1871–1986) is adopted from Parthasarathy (1987), which was originally computed from the monthly rainfall data of about 3000 raingages by weighting the areas of the different meteorological subdivisions of India (Parthasarathy and Mooley, 1978).

Monthly mean zonal wind anomalies at 700 mb and 200 mb for the 17 years (1968–1984) are adopted from the National Meteorological Center (NMC)'s operational tropical wind field analysis. Since the wind data at 850 mb and the surface do not adequately cover the analysis period, we utilized the wind field at 700 mb as representative of the lower troposphere. The validity of this assumption is discussed in Yasunari (1985). Monthly mean outgoing longwave radiation (OLR) data compiled at NMC for the period from 1974 to 1984 are also used. The anomalies of each parameters described here are computed simply by subtracting the mean monthly value, which is obtained by averaging the all available data.

3. Indian Monsoon and SST in the Pacific Basin

Figure 1 shows the lag-correlations between the ISM rainfall and the SST anomalies for wider areas in the equatorial western and eastern Pacific. To deduce the relationships for seasonal means, the SST data are smoothed by three-months moving average. Y(0) denotes the year of the summer monsoon referenced. It is noteworthy that the correlations of SST to ISM rainfall gradually increase from the summer of Y(0) to the following winter, and reach the maximum (minimum) in January or February of Y(+1) in the western (eastern) Pacific. Particularly in the western Pacific, the maximum value of the correlation coefficient reaches +0.79, which is far above the 99% confidence level. Relatively high values with opposite signs to Y(0) are also found in the summer and fall months (June to November) of the year before (Y(−1)), though these values are not as significant as those of the Y(0)/Y(+1) winter. This secondary maximum (or minimum) of correlation in Y(−1)

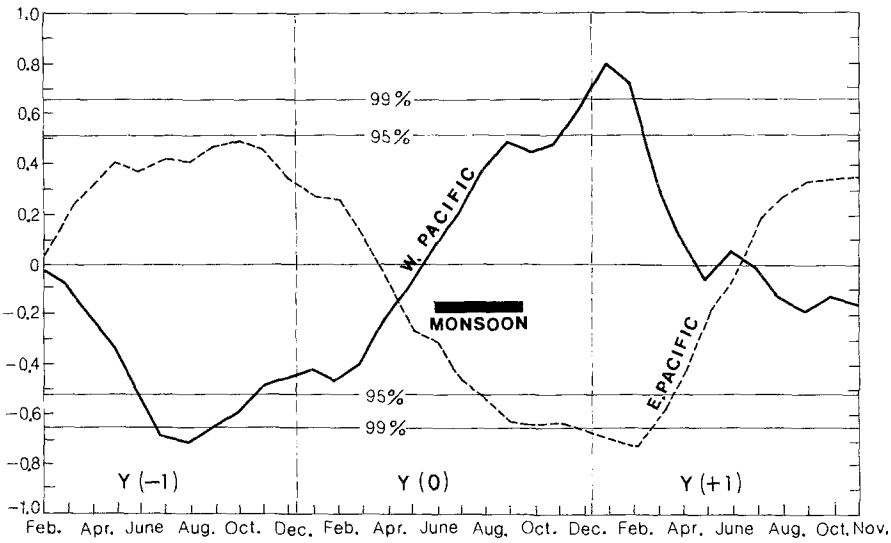

Fig. 1. Lag-correlations between Indian monsoon rainfall and sea surface temperature in the western (0°–8 °N, 130 °E–150 °E) and the eastern (0 °–8 °N, 170 °W–150 °W) Pacific. The reference monsoon season is shown with thick black bar. Y(0) denotes the year of reference monsoon and Y(−1) (Y(+1)) denotes the year before (after) the reference monsoon year

seems to be due to the strong biennial nature of both ISM rainfall (Bhalme and Jadhav, 1984) and SST in the equatorial Pacific (Yoshino and Kawamura, 1987; Meehl, 1987).

Figure 2 shows the spatial pattern of lag-correlations between the ISM rainfall and the SST anomalies for the (a) winter of Y(−1)/Y(0), (b) summer of Y(0) and (c) winter of Y(0)/Y(+1). Systematic changes in correlation patterns can be seen from the preceding winter to the following winter. The change of sign between the western and the eastern Pacific is noticeable particularly along the equatorial belt. The overall pattern is most significant in the winter of Y(0)/Y(+1), and is very similar to the SST anomaly pattern for the typical El Niño phase (e.g., Rasmusson and Carpenter, 1982). However, it should also be noted that the positive correlations in the western Pacific are as significant as the negative correlations in the central through the eastern Pacific, which is not obvious from the real SST anomaly pattern. The pattern for the summer of Y(0) is similar to that for the winter of Y(0)/Y(+1), but the values as a whole are not as significant. Thus, the SST anomalies in the tropical Pacific, particularly in the western part are closely associated with Indian monsoon activities in such manner that SST follows the monsoon with a lag of one to two seasons.

In the subtropical western Pacific and along the east coast of the Asian continent, a narrow area of negative correlations is found in the winter of Y(0)/Y(+1), which is not seen in the summer of Y(0) (Fig. 2(b)). This anomalous pattern seems to be closely related to the effect of anomalous winter monsoon surges from Siberia to areas of SST anomalies in the northwest Pacific, as discussed by Kawamura (1986) and Hanawa et al. (1988). If this is the case, then there should be a significant association between the Asian summer monsoon activity and the following Asian winter monsoon activity.

4. Indian Monsoon and SWT in the Western Pacific

The SWT anomalies may represent more adequately the measure of heat content anomalies in the oceanic mixed layer. This is true particularly in the western Pacific, where variances of SST anomalies are small compared to those in the eastern Pacific. Figure 3 shows the vertical time section of SWT anomalies from the surface to 800 m depth averaged from 2 °N through 10 °N along the longitude line of 137 °E. A remarkable feature is that the anomalies show a nearly in-phase fluctuation through the whole mixed layer. The maximum variance occurs at 100 m through 200 m depth, which corresponds to the main thermocline. Another feature to be noted in this diagram is the distinct biennial nature of the anomalies.

The lagged-correlations between the ISM rainfall and SWT anomalies averaged for the surface mixed layer (0–30 m) are shown in Table 1. The most significant correlation appears in January of Y(+1) with a value of 0.83, whereas relatively high negative correlations are also seen in the pre-

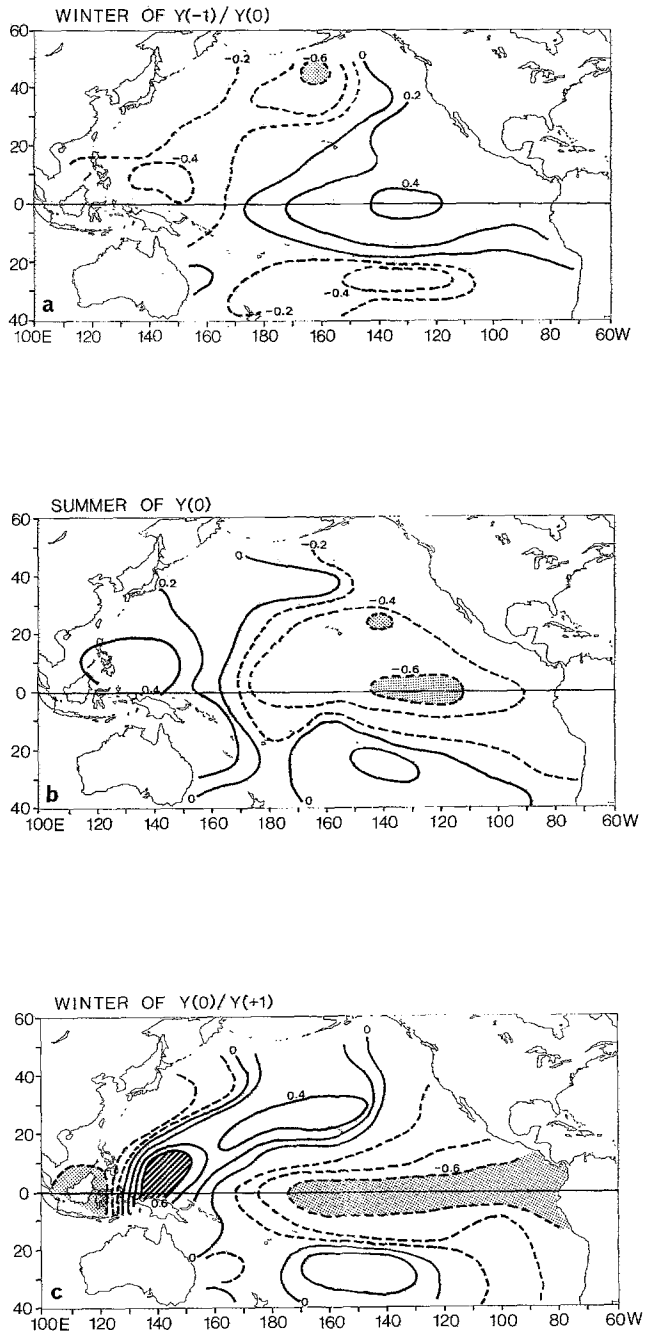

Fig. 2. Spatial distribution of lag correlation between the Indian monsoon rainfall of Y(0) and sea surface temperature anomalies for (a) preceding winter (DJF), (b) contemporary summer (JJA) and (c) following winter. Positive (negative) values of more (less) than 0.6 (−0.6) are shaded (stippled)

ceding seasons (July of Y(−1) and January of Y(0)) with a minimum value of −0.75. These results are consistent with those from the SST data (Fig. 1).

The vertical profile of the correlations between the ISM rainfall and the SWT anomalies of July (Y(0)) plus January (Y(+1)) of each depth is shown in Fig. 4. High positive correlations exceeding the 99% confidence level are found in the layer above 300 m depth, which roughly corresponds to the bottom of main thermocline of this latitude zone (2 °N–10 °N) (Kurihara, 1985). The maximum correlation (nearly 0.80) appears at 10 to 20 m depth, e.g., the core layer of the surface mixed layer, while the second maximum exists at the core layer of the main thermocline (about 150 m), where the variance of the SWT anomalies appears to be maximum (see Fig. 3).

The time series of ISM rainfall anomalies are compared to the SWT anomalies at 20 m and 100 m in the following January, as shown in Fig. 5. It is obvious from this figure that the strong (weak) summer monsoons are followed by the positive (negative) SWT anomalies. It is also evident that these two time series show the quasi-biennial oscillation, which may be responsible for the secondary maxima in the correlations between the ISM rainfall and the SST and SWT in the preceding summer through winter (Fig. 1 and Table 1).

5. Indian Monsoon and Tropical East-West Circulation

The results of lag correlations between ISM rainfall and SST and SWT in the tropical Pacific suggest that the strong convective activities over south Asia through the central Pacific associated with the active Indian summer monsoon may cause the "piling up" of warm surface waters over the tropical western Pacific to the east of the Philippine islands, via a strong tropical east-west circulation (Krishnamurti, 1971). The oceanic process for the piling up of warm water by strong surface easterly wind stress is discussed by White et al. (1987) and others. What is crucial for the evolution of SST and SWT anomalies over the Pacific, as shown in Fig. 1 and Fig. 2, is that the strong easterly wind stress over the western Pacific should be maintained or further intensified throughout the seaons from the norther summer to the following winter. This feature is clearly shown in the lag correlation diagram between ISM rainfall and zonal wind anomalies in the upper (200 mb) and the lower (700 mb) troposphere along the equatorial belt (5 °N–5 °S) as shown in Fig. 6. At 700 mb (Fig. 6 (a)), negative correlations are significantly high

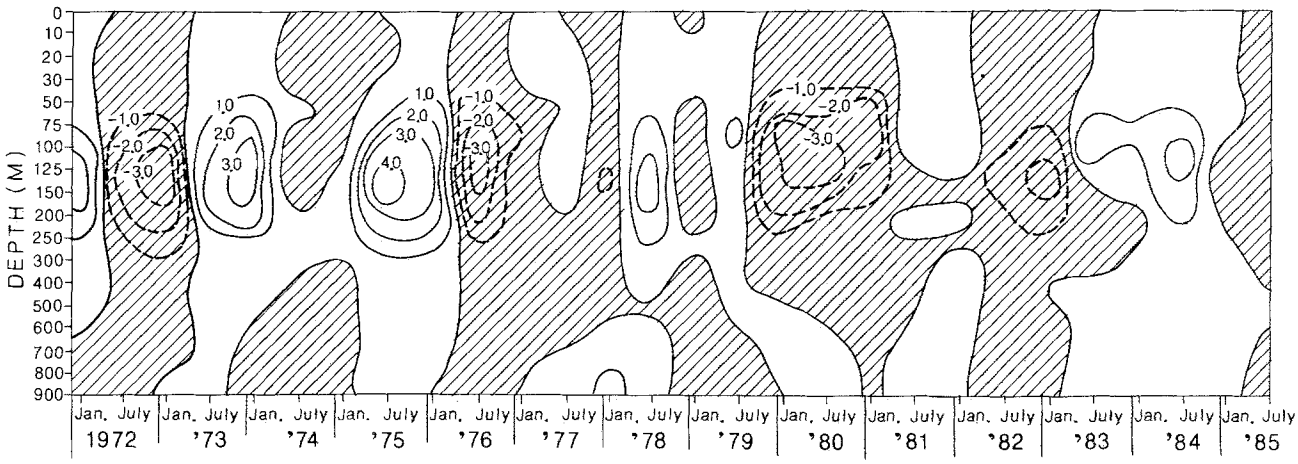

Fig. 3. Vertical time section of January and July sea water temperature anomalies from the surface to 800 m depth averaged for the 137 °E line from 2 °N to 10 °N

Table 1. *Lag-Correlations Between Indian Monsoon Rainfall and Sea Water Temperature Anomalies Averaged for Surface Mixing Layer (0 to 30 m) of the Western Pacific*

Y(−1)		Y(0)		Y(+1)	
Jan.	Jul.	Jan.	Jul.	Jan.	Jul.
−0.49	−0.61	−0.75	−0.22	−0.83	−0.10

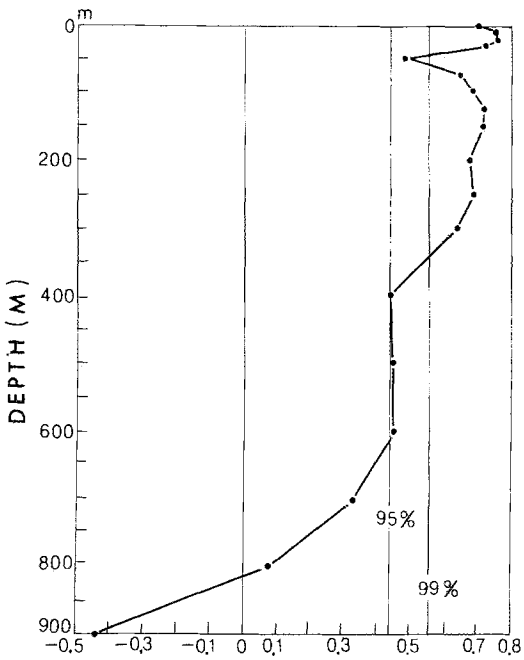

Fig. 4. Vertical profile of correlations between Indian monsoon rainfall and sea water temperature anomalies averaged for July of Y(0) and January of (+1)

(more than 0.7), particularly between 150 °E and 180 °E from the summer monsoon season of Y(0) through the following winter. Over the eastern Indian Ocean through the Indonesian maritime continent (90 °E to 130 °E), in contrast, positive correlations are seen. A similar correlation pattern, but with the opposite sign, can be seen in the summer of Y(−1) through the winter of Y(−1)/Y(0) associated with the QBO nature of the tropical atmosphere, though the pattern is less significant. At 200 mb (Fig. 6 (b)), the overall correlation pattern is very similar to, or even more systematic than, that of 700 mb except with the opposite sign. Again, the maximum east-west contrast of correlation appears in the winter of Y(0)/Y(+1), when the absolute coefficient values exceeds 0.7 both in the western and the eastern Pacific. These timelag-correlation diagrams also show the eastward propagation of correlation pattern from the Indian Ocean side toward the eastern Pacific from Y(0) through Y(+1), which corresponds to the eastward propagation of the tropical anomalous east-west circulation in the QBO time scale (Yasunari, 1985).

The anomalous east-west circulations suggested above should be associated with the anomalous large-scale convection over the Asian monsoon region through the equatorial Pacific in the seasonal cycle starting from the Indian monsoon season. This features is demonstrated in Fig. 7, where

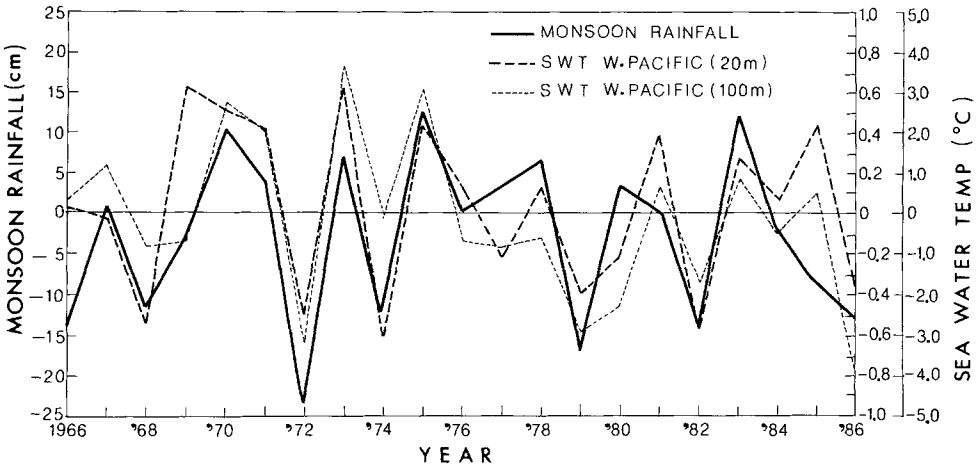

Fig. 5. Time series of Indian monsoon rainfall anomalies (thick solid line) and sea water temperature anomalies at 20 m (thick dashed line) and 100 m (thin dashed line) depth averaged for the 137 °E line (2 °N–10 °N) in the succeding January

the anomalous OLR and 700 mb wind fields are seasonally composited in reference to the strong monsoon years. Since the OLR data is available only after 1974, only 4 strong monsoon years (1975, 1978, 1981, 1983) are composited in this case. However, the anomalous wind field composited for 6 strong monsoon years (not shown) appeared to be substantially the same pattern as Fig. 7. In March-April-May (MAM) of the strong summer monsoon year (Fig. 7 (a)), convection is relatively strong in the central through the eastern Pacific, whereas it is still weaker than normal in the western Pacific. The anomalous wind field along the equator is consistent with this anomalous OLR field. Thus, the large westerly anomalies with anomalous convergence are noticeable in the eastern Pacific, whereas the anomalous divergence is apparent near the positive anomalies of OLR in the western Pacific. It is also of interest to note that the OLR anomalies are positive along the South Pacific Convergence Zone (SPCZ).

In June-July-August (JJA) (Fig. 7 (b)), the OLR field drastically changes from the previous season. The negative anomalies (stronger convection) appear over India through southeast Asia, and the positive anomalies (weaker convection) in the western Pacific become less significant and shift their position more eastward. The area of negative anomalies in the eastern Pacific is considerably diminished. A notable change in the wind field is the appearance of easterly anomalies over the central and the eastern Pacific. The anomalous southwesterlies over the Arabian sea are manifested as stronger monsoon flows.

In September-October-November (SON) of the strong ISM year (Fig. 7 (c)), the negative OLR anomalies further develop and extend the areas over southeast Asia throuth the equatorial western Pacific, while the positive anomalies over the central/eastern Pacific also develop. Associated with this east-west contrast of OLR anomalies is the further intensification of easterly anomalies along the equatorial Pacific.

In December-January-February (DJF) (Fig. 7 (d)), the overall feature in the anomalous OLR and wind field is very similar to that in SON, or is further developed. An area of negative OLR anomalies is also developed over SPCZ and South America, wshich suggest the intensified tropical east-west circulation along the Indian Ocean through the South American sector. It should be noted that at this stage the SST (SWT) anomalies reach their maxima in the western Pacific while they reach their minima in the eastern Pacific (Table 1 and Fig. 2). These anomalous patterns in OLR and wind field established in SON through DJF of strong ISM year continue through MAM of the post strong ISM year (Fig. 7 (e)), though the anomalies are to some extent diminished as a whole. These patterns are, however, completely collapsed or changed to the opposite pattern by the start of the next Indian summer monsoon as suggested in the change from Fig. 7 (a) to Fig. 7 (b). In the composites of weak ISM year, only

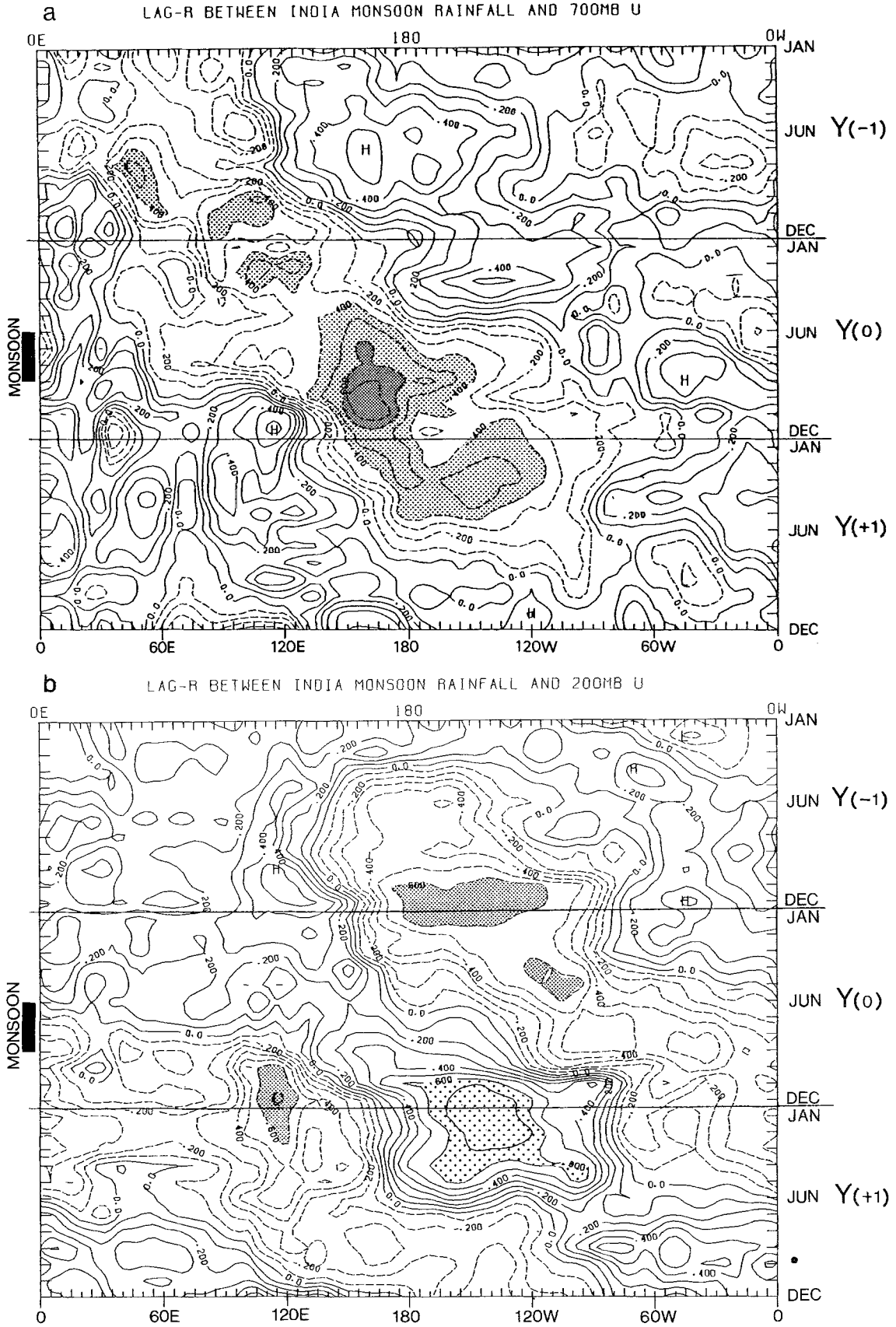

Fig. 6. Time lag − longitude section of correlation coefficients between Indian monsoon rainfall and zonal wind at (a) 700 mb and (b) 200 mb along the equatorial belt (5 °N–5 °S). Units are 0.2. Negative values are shown with dashed lines. Positive (negative) values of more (less) than 0.4 (−0.4) (0.6 and −0.6 for (b)) are dotted (shaded). Positive (negative) values of more (less) than 0.6 (−0.6) in (a) are dark shaded

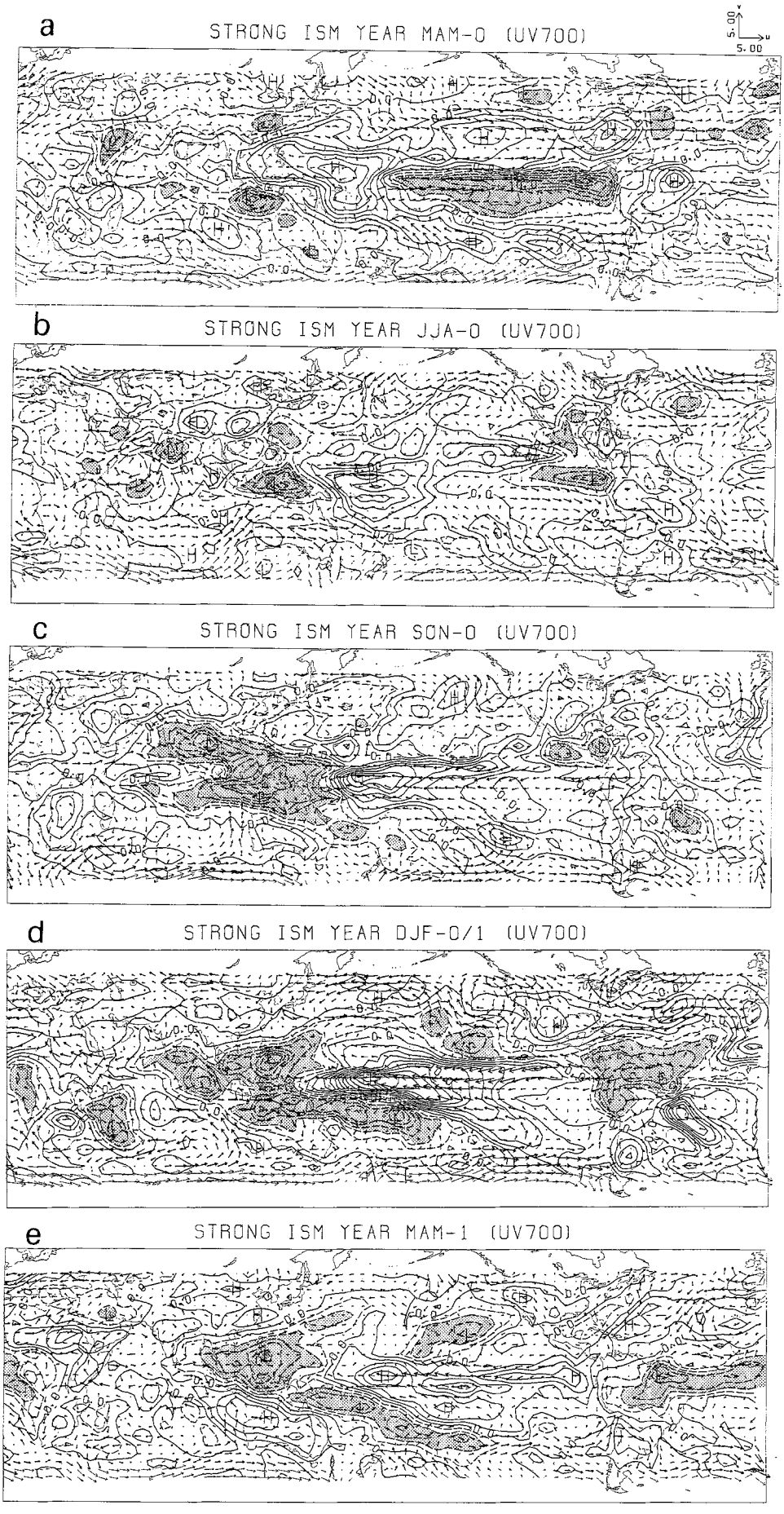
a
STRONG ISM YEAR MAM-0 (UV700)
5.00
5.00
b
STRONG ISM YEAR JJA-0 (UV700)
c
STRONG ISM YEAR SON-0 (UV700)
d
STRONG ISM YEAR DJF-0/1 (UV700)
e
STRONG ISM YEAR MAM-1 (UV700)

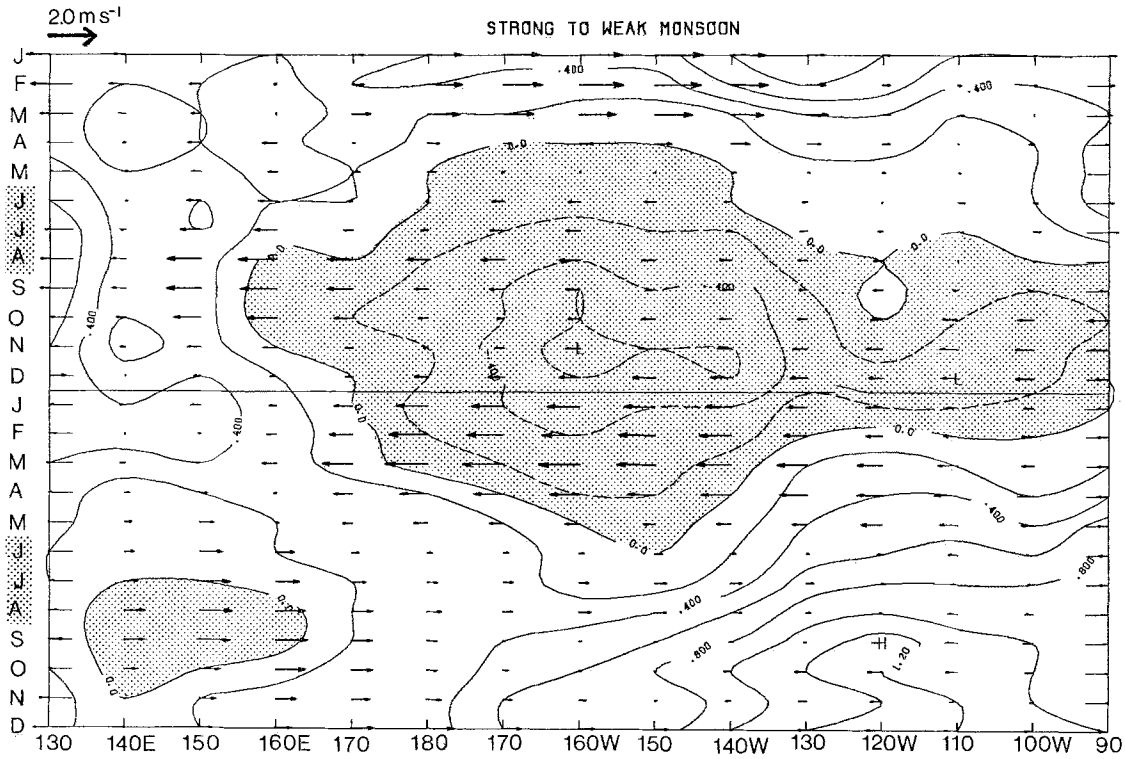

Fig. 8. Longitude-time section of anomalous SST and zonal wind at 700 mb along the equator composited for two years from strong ISM year to weak ISM year. Positive (negative) values in SST field are shown with solid (dashed) lines (unit: 2.0 C) and negative values are stippled

mirror images (i.e., very similar patterns but with opposite signs both in OLR and wind field) of Fig. 7 are found (not shown).

Thus, a stronger (weaker) than normal Indian monsoon is most probably followed by stronger (weaker) easterly wind over the central Pacific and stronger (weaker) westerly wind to the west of 130 °E, i.e., stronger (weaker) low-level convergence over the equatorial western Pacific during the succeding autumn and winter. This means that the anomalies of some atmospheric parameters first appear over the Indian monsoon region and move towards the equatorial central Pacific, through the seasonal migration of convection center from the norther summer to the northern winter and spring. This characteristic nature of the interannual variability in the tropics was also substantiated by Meehl (1987).

6. SST/Zonal Wind Relations Along the Equatorial Pacific

In the previous sections, the evidence was shown that the SWT anomalies in the western Pacific and the SST anomalies in the whole tropical Pacific are well correlated with the preceding ISM activities. This correlation was also suggested to be physically based on the characteristic nature of anomalies in convection and associated circulation field over the Asian monsoon region through the tropical Pacific, which start from the northern summer and persist up to the end of the succeding winter or spring.

To further examine how the atmosphere and ocean are coupled to each other along the equatorial Pacific associated with the ISM and the seasonal cycle, the zonal wind anomalies at 700 mb

Fig. 7. Composites of anomalous OLR and anomalous wind at 700 mb for (a) March-April-May, (b) June-July-August, (c) September-October-November, (d) December-January-February of strong ISM year and (e) March-April-May of the year next. Positive (negative) values in OLR field are shown with solid (dashed) contours (unit: 2.0 $W m^{-1}$) and negative values less than −4.0 are stippled

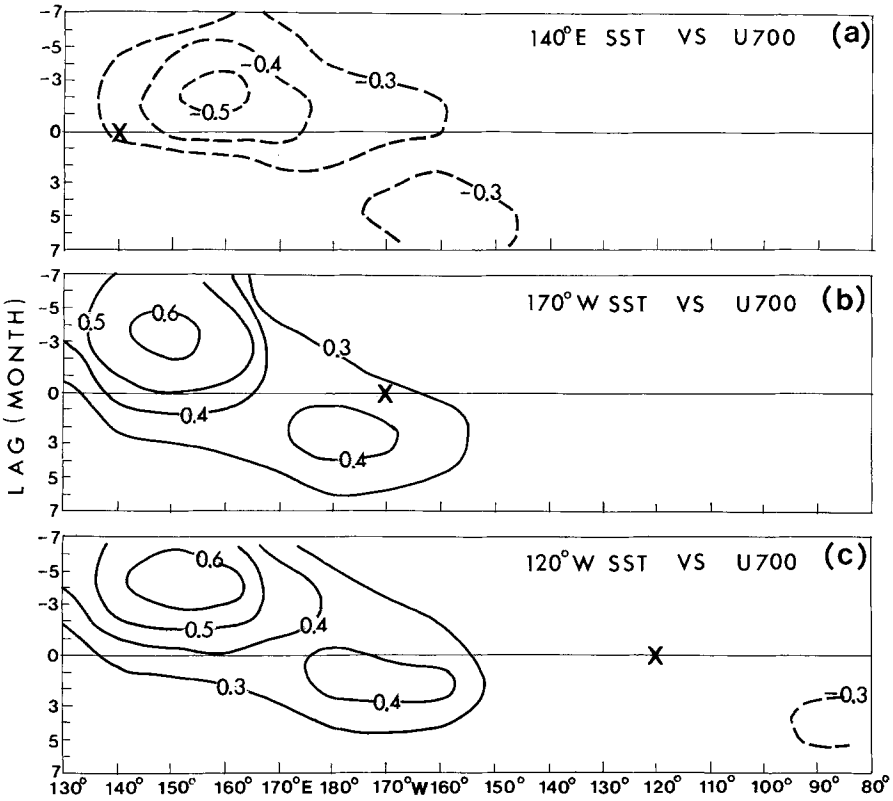

Fig. 9. Lag-correlations between 700 mb zonal wind anomalies along the equator and SST anomalies at (a) 140 °E, (b) 170 °W and (c) 120 °W at the equator. Contours of more (less) than 0.3 (−0.3) are shown with solid (dashed) lines (unit: 0.1). Negative lags imply that zonal wind leads SST

and SST anomalies are composited in reference to the ISM activity. The important parameters for the atmosphere/ocean interaction in the equatorial Pacific are zonal wind and OHC of the surface layers (Cane et al., 1986; Wyrtki, 1985; Yamagata and Masumoto, 1989; etc.). Strictly speaking, the mean SWT of the surface layer, instead of SST, should be used as a measure of OHC in the oceanic mixed layer. In the eastern Pacific, where the mixed layer depth is far smaller and its variability is far larger than those in the western Pacific, SST anomaly is supposed to be a good measure of OHC anomaly. The correlations between the observed mean mixed layer temperature at 160 °W and 100 °W along the equatorial belt adopted from Meyers et al. (1988) and the SST at the same points used here are certainly proved to be very high (e.g., 0.89 and 0.93, with number of freedom of about 60). In the western Pacific, where the large OHC is sustained by the combined effect of radiation balance of the surface, horizontal advection and down- or up-welling, it may generally be supposed that SST anomaly does not necessarily represent OHC anomaly. However, the SWT temperature anomalies, which show nearly in-phase fluctuation from the surface to the bottom of the mixed layer as shown in Fig. 3, strongly suggest that even in the western Pacific the SST anomaly may well reflect the OHC anomaly as far as a proper spatial and time average is applied. We have tentatively concluded, therefore, that SST anomaly adopted here is a good measure of OHC anomaly in the surface mixed layer.

Figure 8 shows a longitude-time section of these two parameters composited for two years, by using 6 cases starting from the strong ISM years (i.e., 1971, 1973, 1975, 1978, 1981 and 1983). Note that in these cases the second years all correspond to weak ISM years including ENSO years. Therefore, the biennial cycles are particularly strong. At nearly the same time when the strong ISM starts, easterly anomalies develop over the whole Pacific basin, particularly in the western Pacific to the west of the dateline. The development of easterly anomalies in the western Pacific from an ISM season to the succeding autumn (September through November) is followed by large negative SST anomalies in the central/eastern Pacific and large positive SST anomalies in the western Pacific in the succeding winter. On the other hand, these negative SST anomalies in the central/eastern Pacific in October through January are followed by

the easterly wind maxima in late winter through the following spring (January through April). In the second year the change from easterly to westerly anomalies seems to be associated with the start of weak ISM. The westerly anomalies are significant again over the longitudes 150 °E to 160 °E in the western Pacific. The composites starting from the weak ISM years (not reproduced here) show just the opposite features to Fig. 8, as is easily supposed from the anomalies of the second year (i.e., weak monsoon year) in Fig. 8.

The relations between zonal wind anomalies and SST evolutions along the equator are more clearly demonstrated in the lag-correlation diagrams between zonal wind anomaly of each longitude in the Pacific basin and SST anomalies of some specified longitudes, as shown in Fig. 9. It is noteworthy to state that not only in the western Pacific, but also in the central/eastern Pacific, SST is significantly correlated to the zonal wind between 150 °E and 160 °E in the western Pacific with a few or several months lag. The signs of correlations are opposite to each other. That means that strong easterly anomalies over these longitudes are largely responsible for producing the positive (negative) SST anomalies to the west (east) several months later, and vice versa. It should be noted here that the correlation of zonal wind with ISM is highest at these longitudes, as shown in Fig. 6. In other words, the anomalous ISM activity is closely associated with zonal wind anomalies over this region possibly through the tropical east-west circulation, which may, in turn, produce SST anomalies with some time lag. We may emphasize here that the wind field of these longitudes leads the SST field over the whole equatorial Pacific.

In the central/eastern Pacific (Fig. 9(b) and 9(c)), the secondary maxima in lag-correlations are also noted, showing that SST leads the zonal wind with a few months. This suggests that the positive feedback process that the SST anomalies, once produced by the wind anomalies, further intensify the anomalous wind field has an additional role on the evolution of the coupled atmosphere/ocean system, particularly during the mature phase of warm or cold events there (Fig. 8).

7. Summary and Remarks

Lag correlation analyses between the ISM rainfall and SST or SWT anomaly in the tropical Pacific show that the interannual fluctuation of the ISM activity with a QBO nature strongly controls the OHC anomaly of the oceanic mixed layer in the tropical Pacific, particularly in the western Pacific. Lag correlations between ISM rainfall anomaly and zonal wind anomaly in the lower troposphere, and that between zonal wind anomaly and SST anomaly along the equator strongly suggest that the OHC anomalies are formed by the anomalous easterly or westerly surface wind stress particularly in the western Pacific (150 °E to 160 °E). Very recently, Kutsuwada (1988) also found that the QBO mode in the surface zonal wind stress field is particularly strong over the tropical western Pacific, even compared to the ENSO mode with about 4-year period.

Generally speaking, lag correlations do not necessarily imply immediate cause and effect relations, particularly in case the correlations show cyclic nature as shown in Fig. 1. However, all the statistical results integrated here can be interpreted consistently with each other, as manifestations of time sequences of the some physical processes. For example, both SST and zonal wind at the equatorial Pacific show remarkably large lagged correlations, compared to lead correlations, with the ISM rainfall, as shown in Fig. 2 and Fig. 6. The time lags between the extreme phases of these two parameters suggested from these correlations are consistent with the systematic lags as shown in Fig. 9. In such a case, it may be reasonable to postulate that in reality the SST and the SWT anomalies in winter may be more directly (or physically) linked to the ISM rainfall anomaly in the preceding summer, rather than in the succeding summer, by means of the persistent anomalous wind field. The seasonal evolutions of anomalous wind and OLR field composited for strong (weak) ISM years (Fig. 7) further substantiate the evidence that these wind anomalies over the tropical Pacific are linked with the anomalous convection over the western Pacific which starts from ISM season and persists through the following winter and spring.

The scenario of the ENSO cycle derived here may be very different from that deduced from some coupled atmosphere/ocean models such as Zebiak and Cane (1987), Battisti (1988) among others, which are based solely on the physics of atmosphere/ocean interaction over the Pacific basin. In these models the ENSO cycle depends on

flowing back of warm (or cold) water westward along the equatorial or off-equatorial latitudes through the western boundary reflection of Rossby waves during the cold (or warm) phase (Cane et al., 1986), where the OHC anomaly fundamentally leads the wind stress anomaly in the equatorial Pacific. These models also suggest that the spreading of positive OHC anomaly in the whole equatorial Pacific basin is important for the preconditioning of the ENSO event, or in other words, the triggering of the unstable ocean/atmosphere coupled mode. In the real system, however, the wind stress anomaly in the western Pacific seems to be essential for producing the OHC anomaly later on in the whole equatorial Pacific, as shown in Fig. 8 and Fig. 9. By using a coupled atmosphere/ocean model, Yamagata and Masumoto (1989) demonstrated that once this condition (or preconditioning) is established the ENSO event evolves automatically. They also suggested that the predictability skill of the ENSO shown by Cane et al. (1986) is essentially based on the instability of this preconditioned state.

We should comment here that although individual ENSO years appear every 3 to 6 years, they are all phase-locked with the phases of the QBO in the SWT anomalies in the western Pacific. For example, as shown in Fig. 3, the first half of each calender year of ENSO events (1986, 1972, 1976, 1982) corresponds to the transition phase from the maximum to the minimum in the SWT and SST anomalies in the western Pacific. In 1974 and 1979, however, although the same transitions occurred in the western Pacific (Fig. 3), El Niño events in the eastern Pacific did not occur. In other words, the variation of OHC anomaly in the western tropical Pacific during winter and spring, which seems to be modulated by the preceding Asian monsoon activity via the anomalous surface wind field, may provide a necessary or at least a very favorable dynamical condition for triggering ENSO events in the eastern Pacific. Masumoto and Yamagata (1989) have recently shown in the coupled model that both the OHC anomaly and the strong westerly wind anomaly in the western Pacific are very essential to produce the preconditioning mentioned above.

In fact, the basic time scale of ENSO cycle may be decided by the heat storage of the whole equatorial Pacific basin and the accumulation rate of warm water in the western Pacific as noted by Wyrtki (1985). The present results strongly suggest that the accumulation rate of warm water and also the timing of the preconditioning are modulated fundamentally by the anomalous surface wind field over the central/western Pacific. This wind field may be part of the coupled land/atmosphere/ocean system involving the Asian monsoon system, rather than of the coupled atmosphere/ocean system over the equatorial Pacific.

An important problem now reserved for future is the mechanism of the QBO in this coupled land/atmosphere/ocean system, which seems to be "intrinsic" to the tropics. The amplitude modulation of this oscillation may actually controls the frequency and intensity of so-called „westerly burst" over the western/central Pacific, which seems to be a key factor for triggering the unstable ocean/atmosphere coupled mode. Further analysis for these problems is currently in progress using long term global data sets.

Acknowledgements

The author would like to thank Dr. T. Yamagata for his helpful comments and discussion. He is also grateful to Dr. K. Kurihara of JMA for providing the SWT data. He is also acknowledged to Dr. R. Kawamura and Mr. S.-F. Tien for computing assistance. Dr. S. Ozaki drafted the figures. This research was financially supported by Grant-In-Aid from the Ministry of Education for 1987, 1988 (No. 62540298) and 1989 (No. 01460055).

References

Angell, J. K., 1981: Comparison of variations in atmospheric quantities with sea surface temperature variations in the equatorial Eastern Pacific. *Mon. Wea. Rev.*, **109,** 230–243.

Barnett, T. P., 1985: Variations near-global sea level pressure. *J. Atmos. Sci.*, **42,** 478–501.

Battisti, D. S., 1988: The dynamics and thermodynamics of a warming event in a coupled tropical atmosphere-ocean model. *J. Atmos. Sci.*, **45,** 2889–2919.

Bhalme, H. N., Jadhav, S. K. 1984: The southern oscillation and relation to the monsoon rainfall. *J. Climatol.* **4,** 509–520.

Cane, M. A., Zebiak, S. E., Dolan, S. C., 1986: Experimental forecasts of El Niño. *Nature,* **321,** 827–832.

Hanawa, K., Watanabe, T., Iwasaka, N., Suga, T., Toba, Y., 1988: Surface thermal conditions in the Western North Pacific during the ENSO events. *J. Meteor. Soc. Japan,* **66,** 445–456.

Kawamura, R., 1986: Seasonal dependency of atmosphere-ocean interaction over the North Pacific. *J. Meteor. Soc. Japan,* **64,** 363–371.

Krishnamurti, T. N., 1971: Tropical east-west circulations during the northern summer. *J. Atmos. Sci.,* **28,** 1342–1347.

Kurihara, K., 1985: Relationship between the surface air temperature in Japan and sea water temperature in the Western Pacific. *Tenki*, **32,** 407–417 (in Japanese)

Kutsuwada, K., 1988: Spatial characteristics of interannual variability in wind stress over the Western North Pacific. *J. Climate*, **1,** 333–347.

Masumoto, Y., Yamagata, T., 1990: The birth and evolution of an eastward propagating air-sea coupled disturbance in an aqua-planet. *Meteorol. Atmos. Phys.*, **44**, 1–9.

Meehl, G. A., 1987: The annual cycle and interannual variability in the tropical Pacific and Indian Ocean regions. *Mon. Wea. Rev.*, **115,** 17–50.

Meyers, G., Donguy, J. R., England, M., Reed, R. K., 1988: The Southern Oscillation and heat storage in the equatorial Pacific Ocean, 1979–1984. Part I: Surface heat fluxes and local storage. Submitted to *J. Marine Res.*

Miyakoda, K., Rosati, A., Gudgel, R., Chao, Y., 1987: Study of the 1982/1983 El Niño and Southern Oscillation with an ocean GCM and observational data. Part I: El Niño Sequence. To be submitted.

Nicholls, N., 1984: Predicting Indian monsoon rainfall from sea-surface temperature in the Indonesia-north Australia area. *Nature*, **307,** 576–577.

Parthasarathy, B., 1987: Droughts/floods in the summer monsoon season over different meteorological subdividions of India for the period 1871–1984. *J. Climatol.* **7,** 57–70.

Parthasarathy, B., Mooley, D. A., 1978: Some features of a long homogeneous series of Indian summer monsoon rainfall. *Mon. Wea. Rev.*, **106,** 771–781.

Pazan, S. E., White, W. B., Inoue, M., O'Brien, J. J., 1986: Off-equatorial influence upon Pacific dynamic height variability during the 1982–1983 El Niño/Southern Oscillation event. *J. Geophys. Res.*, **91,** 8437–8449.

Philander, S. G. H., Yamagata, T., Pacanowski, R. C., 1984: Unstable air-sea interactions in the tropics. *J. Atmos. Sci.*, **41,** 604–613.

Rasmusson, E. M., Carpenter, T. H., 1982: Variations in tropical sea surface temperature and surface wind fields associated with the Southern Oscillation/El Niño. *Mon. Wea. Rev.*, **110,** 354–384.

Rasmusson, E. M., Carpenter, T. H., 1983: The relation between eastern equatorial Pacific sea surface temperature and rainfall over India and Sri Lanka. *Mon. Wea. Rev.*, **111,** 517–528.

Shukla, J., Paolino, D. A., 1983: The Southern Oscillation and long-range forecasting of the summer monsoon rainfall over India. *Mon. Wea. Rev.*, **111,** 1830–1837.

Walker, G. T., Bliss, E. W., 1932: World Weather V. *Mem. Roy. Met. Soc.*, **4,** 53–84.

White, W. B., Pazan, S. E., Inoue, M., 1987: Hindcast/Forecast of ENSO events based upon the redistribution of observed and model heat continent in the Western Pacific. *J. Phys. Oceanogr.*, **17,** 264–280.

Wyrtki, K., 1975: El Niño – The dynamic response of the equatorial Pacific Ocean to atmospheric forcing. *J. Phys. Oceanogr.*, **5,** 572–584.

Wyrtki, K., 1985: Water displacements in the Pacific and the genesis of El Niño cycles. *J. Geophys. Res.*, **90,** 7129–7132.

Yamagata, T., Masumoto, Y., 1989: A simple air-sea coupled model of the origin of a warm ENSO event. To appear in *Phil. Trans. Roy. Soc.*

Yasunari, T., 1985: Zonally propagating modes of the global east-west circulation associated with the Southern Oscillation. *J. Meteor. Soc. Japan*, **63,** 1013–1029.

Yasunari, T., 1987: Global structure of the El Niño/Southern Oscillation. Part II. Time evolution. *J. Meteor Soc. Japan*, **65,** 81–102.

Yoshino, M., Kawamura, R., 1987: Periodicity and propagation of sea surface temperature fluctuations in the equatorial Pacific. *Beitr. Phys. Atmos.*, **60,** 283–293.

Zebiak, S. E., Cane, M. A., 1987: A model El Niño-Southern Oscillation. *Mon. Wea. Rev.*, **115,** 2262–2278.

Authors address: Tetsuzo Yasunari, Institute of Geoscience, University of Tsukuba, Tsukuba, Ibaraki 305, Japan.